Journal of Physics: Conference Series **1596** (2020) 012037 doi:10.1088/1742-6596/1596/1/012037

Progress Towards Laser Wakefield Acceleration and Applications at the Scottish Centre for the Application of Plasma-based Accelerators (SCAPA)

G K Holt[1], G Battaglia[1], E Brunetti[1,2], J Feehan[1], A Kornaszewski[1], W Li[1], A Maitrallain[1], G G Manahan[1], W D Pring[1], L R Reid[1,2], M Shahzad[1], R Spesyvstev[1], G Vieux[1], S M Wiggins[1] and D A Jaroszynski[1]

[1]Scottish Universities Physics Alliance, Department of Physics, University of Strathclyde, Glasgow, G4 0NG, UK

[2]The Cockcroft Institute, Sci-Tech Daresbury, Keckwick Lane, Daresbury, Warrington, WA4 4AD, UK

E-mail: george.holt@strath.ac.uk

E-mail: d.a.jaroszynski@strath.ac.uk

Abstract. Laser wakefield accelerators (LWFAs) are promising sources of high brightness particle and radiation beams with many possible applications, ranging from scientific research to medicine, industry and border security. The Scottish Centre for the Application of Plasma-based Accelerators (SCAPA) is a university-based facility employing the use of two high-power, ultrashort pulse lasers to advance research, development and application of laser-plasma accelerators. Here we report on recent advancements in LWFA research at SCAPA and upcoming research programmes to demonstrate proof-of-concept applications of the LWFA.

1. Introduction

Recent developments of high-power, ultrashort pulse lasers are driving technological development in a broad range of fields that require electromagnetic and particle radiation sources. One method of producing a tuneable, high peak brightness radiation source is using a laser wakefield accelerator (LWFA), which complements conventional accelerators based on radio-frequency (RF) or microwave cavities. Their comparatively low footprint and capital cost makes them accessible to universities, industry and medical facilities.

It has been demonstrated that the µm-scale accelerating structures generated by the LWFA can accelerate electrons up to 8 GeV in centimetres [1]. The resulting beams are useful for studying high-field quantum electrodynamics [2, 3] and as sources at large-scale particle collider facilities [4]. They may also be converted to X-rays via bremsstrahlung for fast imaging of dense materials [5, 6, 7], or used to generate medical isotopes [8]. Betatron radiation produced by transverse oscillation of electrons within a cavitated wake can generate X-rays with energies in the keV to MeV range [9], and also be used for non-destructive projection microscopy [10], microcomputed tomography [11] and single-shot phase contrast imaging [12] of biological specimens.

The Scottish Centre for the Application of Plasma-based Accelerators (SCAPA), at the University of Strathclyde, UK, is a university-based facility dedicated to research, development and application of laser-driven particle accelerators and associated radiation sources. It comprises two high-power laser systems and seven permanent beamlines, each designed to exploit particle accelerators or investigate laser-plasma interactions. The centre is well set up for investigating novel applications of high-power lasers and the radiation resulting from their interaction with matter.

This paper gives an overview of the facilities at SCAPA that are pertinent to LWFA and presents recent characterisation and commissioning of the lasers. Future projects are also outlined and discussed.

2. SCAPA Infrastructure

The centre is laid out over two levels. Two high power laser labs are situated on the first floor alongside preparation and analysis labs, which house fume cupboards, sealed sources, biological equipment, image plate readers, target metrology stations, etc. Both high power lasers are commercial Ti:sapphire systems. One delivers 350 TW at up to 5 Hz, while the other delivers 40 TW at up to 10 Hz.

High power laser pulses are transported, after compression, in vacuum through the floor of the laser lab to one of the radiation shielded concrete bunkers on the ground floor via a junction box, which selects the target beamline, as shown in figure 1. The 40 TW laser delivers high power pulses to beamlines in bunkers A and C, while the 350 TW delivers pulses to beamlines in bunkers A and B. Concrete shielding doors on pneumatic sleds, shown in figure 2, enable access to each of the bunkers and can be rapidly closed for full power operation. The bunkers and high power laser labs are vibrationally isolated to reduce pointing fluctuations. Bunker B is dedicated to laser-solid interaction experiments.

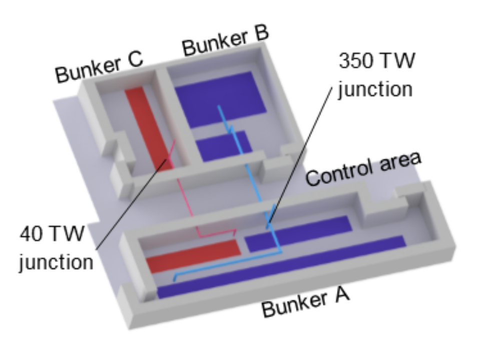

Figure 1. Ground floor layout of SCAPA showing the laser-driven beamlines. Red beam paths are serviced by the 40 TW laser and blue beam paths by the 350 TW laser.

Figure 2. The floating concrete door and entrance to the shielded bunker C.

3. Laser Drivers

Two commercial high-power Ti:sapphire laser systems act as the laser sources at SCAPA. The compressed pulse from each system is transported to a particular beamline in the bunkers depending on the laser power required. This enables simultaneous operation of two beamlines, whilst staff in the other bunker can carry out preparatory or maintenance work.

Journal of Physics: Conference Series **1596** (2020) 012037 doi:10.1088/1742-6596/1596/1/012037

3.1. 350 TW *System*

The 350 TW laser was designed and manufactured by Thales Optronique [13] and commissioned in 2017. At that time, it was the highest average power laser, in its class, in the world [14]. Laser parameters measured in the class 1000 ISO 6 clean room are given in table 1. A photograph of the system is shown in figure 3. A variable 10% – 100% transmission attenuator is used after the final amplifier to adjust the energy delivered to the target areas.

Table 1. 350 TW laser specifications.

Parameter		**Value**
Repetition rate		5 Hz
Central wavelength ± FWHM bandwidth		800 nm ± 28 nm
FWHM compressed pulse duration		33 fs
Strehl ratio		> 0.85
Collimated beam diameter		125 mm
Pulse energy	after compression	8.75 J
	at output of final amplifier	14 J
Contrast ratio		10^{10} : 1 @ 100 ps 10^{8} : 1 @ 30 ps 10^{4} : 1 @ 2 ps
Energy stability		$<$ 1.2% rms (500 shots) $<$ 1.5% rms (8 hours)

Figure 3. 350 TW laser system that currently drives four of the SCAPA beamlines.

3.2. 40 TW *System*

The 40 TW laser was originally designed by Amplitude Technologies [15] and has been operational since the Advanced Laser Plasma High-energy Accelerators towards X-rays (ALPHA-X) [16, 17] project began in 2002. Several upgrades have been implemented since then to improve thermal management and energy and pointing stability of the system, including the use of Saga HP pump lasers supplied by Thales as an upgrade to the final amplifier to deliver 1.9 J. A summary of parameters is given in table 2.

Table 2. 40 TW laser specifications.

Parameter		**Value**
Repetition rate		10 Hz
Central wavelength ± FWHM bandwidth		800 nm ± 26 nm
FWHM compressed pulse duration		36 fs
Collimated beam diameter		40 mm
Energy stability		< 1.6% rms (1 hour)
Pulse energy	after compression	1.3 J
	at output of final amplifier	1.9 J

4. Target Areas

Two beamlines dedicated to LWFA at SCAPA are being commissioned. They are located in different bunkers and driven by independent laser systems, which enables the two beamlines to be run simultaneously. They are close to achieving operational parameters. Recent developments towards this goal are presented here for each bunker.

4.1. Bunker C

The first beamline in bunker C is a reconstruction of the ALPHA-X beamline, which predates SCAPA by fifteen years. Much of the equipment (vacuum chambers, electron and photon spectrometers, cameras, etc.) has been redeployed from the previous experimental setup, which is being continually refreshed to ensure it remains state of the art.

An AKA Optics deformable mirror [18] and Phasics wavefront sensor [19] have been implemented to correct optical aberrations introduced during amplification, compression and beam transport. Due to the compact nature of the ALPHA-X beamline, a mirror with a 6 mm hole deflects the beam to a spherical focusing mirror which focusses the beam through the hole to the interaction point. Optimisation to correct focal spot aberrations has been successfully implemented. A 77 cm focal length spherical mirror is used to focus the laser pulse to a spot of FWHM diameter $32.1 \times 32.7\,\mu\mathrm{m}^2$ in a gas target. The pointing stability is $7.5 \times 7.4\,\mu\mathrm{rad}^2$ in $x \times y$.

Pressure regulated gas lines allow for dynamic control of the backing pressure for supersonic gas jets. Wavefront sensor-based gas target metrology [20] is used to determine the plasma density offline (also to be installed as an online diagnostic), with typical density of order $1 \times 10^{19}\,\mathrm{cm}^{-3}$. The plasma channel created by the laser pulse is imaged from the top and side by CCD cameras fitted with objective lenses. A Newport 77480 [21] imaging spectrometer images the plasma channel and side- and back-scattered laser light is collected by optical fibres and sent to VIS-NIR spectrometers.

A 210 mm, 0.7 T dipole magnet mounted on a motorised stage can be placed in the path of the electron beams to disperse the beam onto a LANEX screen, which is used to measure electron energy spectra, currently up to 200 MeV. An electromagnetic quadrupole triplet can be used to focus the electron beam into another electron spectrometer with a resolution better than 1% for $76 - 227$ MeV electrons. The scintillating screens of the spectrometers are imaged with objective lenses and CCD cameras. Several on-axis LANEX screens at various distances from the gas target can be inserted into the beam to measure the transverse spatial profile. The quadrupole triplet can also focus the electron beam into two, 100-period, 1.5 m, 0.27 T undulators to produce radiation in the $70 - 260$ nm wavelength range [22]. X-ray cameras capable of single photon counting [23, 24] are used with X-ray filters, Ross filter pairs and XUV spectrometers to diagnose X-rays produced during the laser-plasma interaction.

The ALPHA-X beamline has demonstrated production of low-emittance [25] and femtosecond [26] duration electron bunches in excess of 100 MeV, in addition to the production of high-charge, wide-angle beams [27]. These results show the capability of this beamline to generate primary and secondary radiation of interest to several research areas. Very high-energy electron (VHEE) beams, in the region of $100 - 200$ MeV has been demonstrated as a novel method of delivering radiation doses to deep-seated tumours [28, 29]. Laser-plasma accelerators may provide an efficient method of treating multiple patients simultaneously by steering the driving beam [30]. Stable MeV nanocoulomb electron beams emitted at wide angles can also be used to generate coherent terahertz radiation with mJ-level energy and encompassing the THz gap [31], which has potential use for studying nonlinear materials, and for industrial and medical imaging [32, 33].

4.2. Bunker A

The 'A2' beamline in bunker A is set up to develop and apply LWFAs. Many of the design decisions stem from experience gained operating the ALPHA-X beamline discussed in the previous section. An image showing the beamline is shown in figure 4.

4 m ($f/32$) and 2 m ($f/16$) off-axis parabolas (OAPs) are available for use to focus the laser beams, matched to user requirements e.g. Rayleigh range and peak intensity. A typical focal spot of the $f/16$ optic is shown in figure 5 with full-width at half-maximum (FWHM) values of

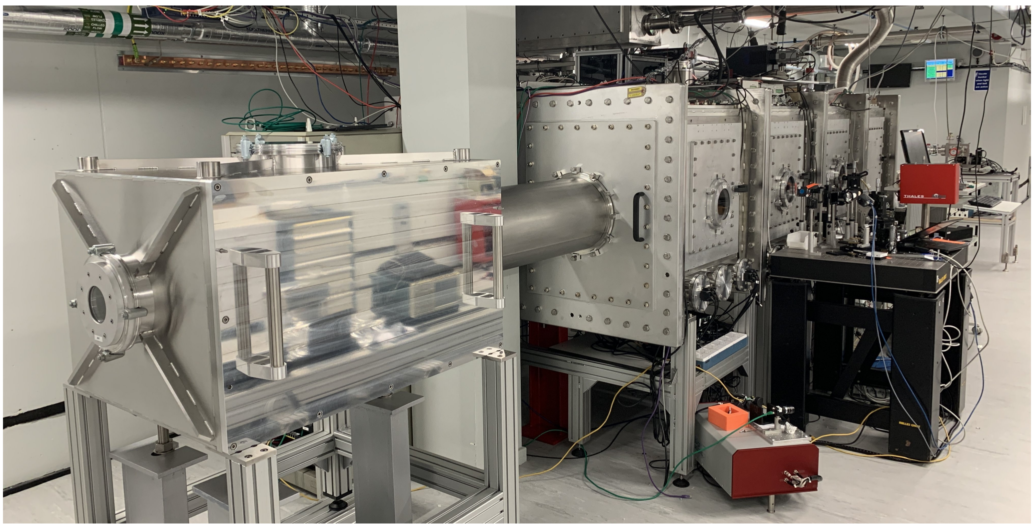

Figure 4. The A2 beamline. The chamber on the left houses a 4 m focusing optic and is connected to the main interaction chamber.

$17.6 \times 19.6\,\mu\mathrm{m}^2$ in $x \times y$. The pointing fluctuation was measured to be $4.4 \times 3.6\,\mu\mathrm{rad}^2$ in the same directions over 200 shots.

Focal spot optimisation after careful alignment of optics is conducted using an ILAO system [34, 35]. A HASO wavefront sensor measures the phase profile of the beam by collecting leakage light from the compressor output. A deformable mirror located immediately before the compressor introduces aberrations to the wavefront that correspond to exactly compensate those measured by the wavefront sensor. Further aberrations introduced during beam transport and focusing are corrected by numerically reconstructing the wavefront from intensity data measurements taken by a focal spot camera and compensating for the aberrations using the deformable mirror.

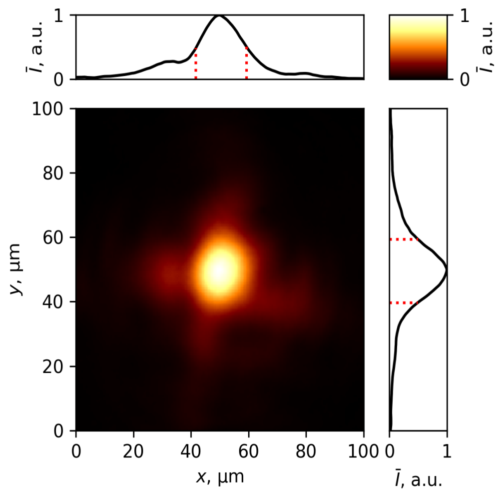

Figure 5. Typical A2 beamline focal spot from the $f/16$ OAP. The colour scale shows normalised fluence. Horizontal and vertical line-outs through the centre of the profile are shown in the subplots, with dashed red lines indicating the position of measurement to acquire a FWHM value in that direction.

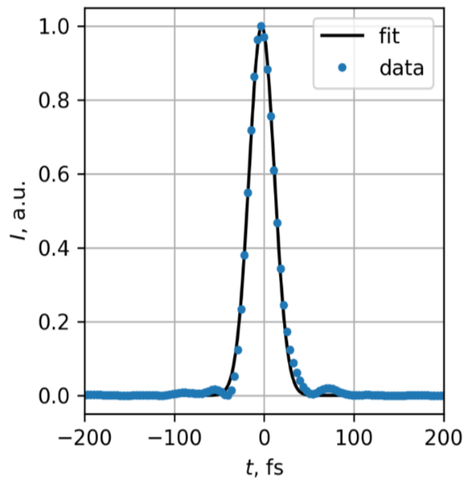

Figure 6. Temporal profile of the 350 TW laser as measured by a Fastlite Wizzler placed as a diagnostic on the A2 beamline. A FWHM value of 33 fs is measured.

A Fastlite Wizzler 800 [36] and FROG [37] are available for temporal intensity and phase measurements and an Amplitude Sequoia [15] and UltraFast Innovations TUNDRA [38] for temporal contrast. A typical Wizzler trace measured in the A2 beamline before the focusing optic, and accounting for the vacuum-air interface window is shown in figure 6. The resulting 33.0 fs FWHM pulse duration obtained was confirmed by FROG measurements in the same location.

The gas target options include a supersonic jet, a variable-length gas cell and a capillary discharge plasma channel. These produce electron beams with energies up to 1 GeV. As in Bunker C, the plasma channel is imaged from the top and side using objective lenses and CCD cameras. An Andor Kymera imaging spectrometer [39] is installed to provide spatially-resolved spectra of the channel. Fibre-coupled VIS-NIR spectrometers are installed to measure the back- and side-scattered laser radiation.

A 0.74 T permanent magnetic dipole is available for use as an electron spectrometer, with an electron beam energy range up to 700 MeV. Despite the similar field strength to the dipole in bunker C, the spectral range is greater due to the larger space afforded by the A2 interaction chamber. Alternatively, a double-dipole magnet will soon be available to provide angularly resolved electron spectra with $\approx$1% resolution at 1 GeV [40]. We have found that commonly available narrow ($\sim$10 nm FWHM) bandpass filters around the region of LANEX peak emission (546 nm) are sufficient to block the scattered laser light from entering the spectrometer cameras.

An adjustable Kirkpatrick-Baez microscope has been designed and installed in the beamline, which is capable of focusing both hard and soft X-rays between 50 eV and 10 keV [41]. With the available X-ray cameras, this can be used to image the X-ray source within the laser-plasma interaction in addition to providing a mm-scale, bright X-ray beam for applications, such as measuring the grain orientation in alloys.

Femtosecond [26] or attosecond [42] electron bunches can be generated by carefully controlling the laser and plasma parameters, which may, in turn, be used to generate ultrashort X-ray pulses. Attosecond XUV radiation pulses with energy between 10 and 100 eV could be produced as attosecond electron bunches oscillate within the plasma bubble in the ion channel [43, 44, 45, 46]. The GeV-scale electron beams produced on the A2 beamline will underpin various research projects. Laser-plasma accelerators may provide an efficient method of producing short-lived medically relevant radioisotopes such as ^{99m}Tc [8] or ^{195m}Pt and will have a sufficiently small footprint and capital outlay to be potential generators at medical facilities. Studies in minimising the 6D emittance of a GeV electron beam will be undertaken towards generating a free-electron laser driver [47, 48].

5. Conclusion

Laser wakefield acceleration is a rapidly developing technology being investigated at a growing number of facilities worldwide, which are dedicated to advancing the field and associated applications. The state-of-the-art facilities at SCAPA make it an ideal location to conduct such research.

6. Acknowledgements

We acknowledge support of the U.K. EPSRC (grant no. EP/K011952/1, EP/J018171/1, EP/N028694/1, EP/J500094/1, EP/P020607/1, EP/R006202/1, EP/T01153X/1), the Scottish Funding Council, the European Union's Horizon 2020 research and innovation programme under grant agreements no. 654148 and no. 871124, Laserlab-Europe, and grant agreement no. 653782, EuPRAXIA.

References

[1] Gonsalves A J, Nakamura K, Daniels J, Benedetti C, Pieronek C, De Raadt T C, Steinke S, Bin J H, Bulanov S S, Van Tilborg J, Geddes C G, Schroeder C B, Tóth C, Esarey E, Swanson K, Fan-Chiang L, Bagdasarov G, Bobrova N, Gasilov V, Korn G, Sasorov P and Leemans W P 2019 *Phys. Rev. Lett.* **122**

[2] Di Piazza A, Müller C, Hatsagortsyan K Z and Keitel C H 2012 *Rev. Mod. Phys.* **84** 1177–1228

[3] Cole J, Behm K, Gerstmayr E, Blackburn T, Wood J, Baird C, Duff M, Harvey C, Ilderton A, Joglekar A, Krushelnick K, Kuschel S, Marklund M, McKenna P, Murphy C, Poder K, Ridgers C, Samarin G, Sarri G, Symes D, Thomas A, Warwick J, Zepf M, Najmudin Z and Mangles S 2018 *Phys. Rev. X* **8** 011020

[4] Esarey E, Schroeder C B and Leemans W P 2009 *Rev. Mod. Phys.* **81** 1229–1285

[5] Edwards R D, Sinclair M A, Goldsack T J, Krushelnick K, Beg F N, Clark E L, Dangor A E, Najmudin Z, Tatarakis M, Walton B, Zepf M, Ledingham K W, Spencer I, Norreys P A, Clarke R J, Kodama R, Toyama Y and Tampo M 2002 *Appl. Phys. Lett.* **80** 2129–2131

[6] Glinec Y, Faure J, Le Dain L, Darbon S, Hosokai T, Santos J J, Lefebvre E, Rousseau J P, Burgy F, Mercier B and Malka V 2005 *Phys. Rev. Lett.* **94**

[7] Cipiccia S, Wiggins S M, Shanks R P, Islam M R, Vieux G, Issac R C, Brunetti E, Ersfeld B, Welsh G H, Anania M P, Maneuski D, Lemos N R, Bendoyro R A, Rajeev P P, Foster P, Bourgeois N, Ibbotson T P, Walker P A, Shea V O, Dias J M and Jaroszynski D A 2012 *J. Appl. Phys.* **111**

[8] Roberts A, Geddes C, Matlis N, Nakamura K, O'Neil J, Shaw B, Steinke S, van Tilborg J and Leemans W 2015 *Appl. Radiat. Isot.* **96** 122–128

[9] Cipiccia S, Islam M R, Ersfeld B, Shanks R P, Brunetti E, Vieux G, Yang X, Issac R C, Wiggins S M, Welsh G H, Anania M P, Maneuski D, Montgomery R, Smith G, Hoek M, Hamilton D J, Lemos N R C, Symes D, Rajeev P P, Shea V O, Dias J M and Jaroszynski D A 2011 *Nat. Phys.* **7** 867–871

[10] Hussein A E, Senabulya N, Ma Y, Streeter M J V, Kettle B, Dann S J D, Albert F, Bourgeois N, Cipiccia S, Cole J M, Finlay O, Gerstmayr E, González I G, Higginbotham A, Jaroszynski D A, Falk K, Krushelnick K, Lemos N, Lopes N C, Lumsdon C, Lundh O, Mangles S P D, Najmudin Z, Rajeev P P, Schlepütz C M, Shahzad M, Smid M, Spesyvtsev R, Symes D R, Vieux G, Willingale L, Wood J C, Shahani A J and Thomas A G R 2019 *Sci. Rep.* **9** 3249

[11] Cole J M, Symes D R, Lopes N C, Wood J C, Poder K, Alatabi S, Botchway S W, Foster P S, Gratton S, Johnson S, Kamperidis C, Kononenko O, Lazzari M D, Palmer C A J, Rusby D, Sanderson J, Sandholzer M, Sarri G, Szoke-Kovacs Z, Teboul L, Thompson J M, Warwick J R, Westerberg H, Hill M A, Norris D P, Mangles S P D and Najmudin Z 2018 *Proc. Natl. Acad. Sci.* **115** 6335–6340

[12] Kneip S, McGuffey C, Dollar F, Bloom M S, Chvykov V, Kalintchenko G, Krushelnick K, Maksimchuk A, Mangles S P, Matsuoka T, Najmudin Z, Palmer C A, Schreiber J, Schumaker W, Thomas A G and Yanovsky V 2011 *Appl. Phys. Lett.* **99**

[13] 2019 Thales Optronics URL `https://www.thalesgroup.com/en/markets/market-specific-solutions/lasers`

[14] Thales 2017 Strathclyde University Acquires one of the World's Most Powerful Lasers from Thales URL `https://www.thalesgroup.com/en/worldwide/group/news/strathclyde-university-acquires-one-worlds-most-powerful-lasers-thales`

[15] 2018 Amplitude URL `https://amplitude-laser.com/`

[16] Jaroszynski D A and Vieux G 2003 Coherent Radiation Sources Based on Laser Plasma Accelerators *AIP Conf. Proc. 6471* (AIP Publishing) pp 902–914

[17] Jaroszynski D A, Bingham R, Brunetti E, Ersfeld B, Gallacher J, Van Der Geer B, Issac R, Jamison S P, Jones D, De Loos M, Lyachev A, Pavlov V, Reitsma A, Saveliev Y, Vieux G and Wiggins S M 2006 *Philos. Trans. R. Soc. A Math. Phys. Eng. Sci.* **364** 689–710

[18] 2012 AKA Optics URL `http://akaoptics.com/`

[19] 2019 Phasics URL `http://phasicscorp.com/`

[20] Plateau G R, Matlis N H, Geddes C G R, Gonsalves A J, Shiraishi S, Lin C, van Mourik R A and Leemans W P 2010 *Rev. Sci. Instrum.* **81** 033108

[21] 2020 Newport URL `https://www.newport.com`

[22] Anania M P, Brunetti E, Wiggins S M, Grant D W, Welsh G H, Issac R C, Cipiccia S, Shanks R P, Manahan G G, Aniculaesei C, Van Der Geer S B, De Loos M J, Poole M W, Shepherd B J, Clarke J A, Gillespie W A, Macleod A M and Jaroszynski D A 2014 *Appl. Phys. Lett.* **104**

[23] Maddox B R, Park H S, Remington B A and McKernan M 2008 Calibration and characterization of single photon counting cameras for short-pulse laser experiments *Rev. Sci. Instrum.* vol 79

[24] Fourment C, Arazam N, Bonte C, Caillaud T, Descamps D, Dorchies F, Harmand M, Hulin S, Petit S and Santos J J 2009 *Rev. Sci. Instrum.* **80**

[25] Brunetti E, Shanks R P, Manahan G G, Islam M R, Ersfeld B, Anania M P, Cipiccia S, Issac R C, Raj G, Vieux G, Welsh G H, Wiggins S M and Jaroszynski D A 2010 *Phys. Rev. Lett.* **105**

[26] Islam M R, Brunetti E, Shanks R P, Ersfeld B, Issac R C, Cipiccia S, Anania M P, Welsh G H, Wiggins S M, Noble A, Cairns R A, Raj G and Jaroszynski D A 2015 *New J. Phys.* **17**

[27] Yang X, Brunetti E, Gil D R, Welsh G H, Li F Y, Cipiccia S, Ersfeld B, Grant D W, Grant P A, Islam M R, Tooley M P, Vieux G, Wiggins S M, Sheng Z M and Jaroszynski D A 2017 *Sci. Rep.* **7**

[28] DesRosiers C, Moskvin V, Bielajew A F and Papiez L 2000 *Phys. Med. Biol.* **45** 1781–1805

[29] Subiel A, Moskvin V, Welsh G H, Cipiccia S, Reboredo D, Evans P, Partridge M, DesRosiers C, Anania M P, Cianchi A, Mostacci A, Chiadroni E, Di Giovenale D, Villa F, Pompili R, Ferrario M, Belleveglia M, Di Pirro G, Gatti G, Vaccarezza C, Seitz B, Isaac R C, Brunetti E, Wiggins S M, Ersfeld B, Islam M R, Mendonca M S, Sorensen A, Boyd M and Jaroszynski D A 2014 *Phys. Med. Biol.* **59** 5811–5829

[30] Kokurewicz K, Brunetti E, Welsh G H, Wiggins S M, Boyd M, Sorensen A, Chalmers A J, Schettino G, Subiel A, DesRosiers C and Jaroszynski D A 2019 *Sci. Rep.* **9**

[31] Yang X, Brunetti E and Jaroszynski D A 2018 *New J. Phys.* **20** 043046

[32] Hafez H A, Chai X, Ibrahim A, Mondal S, Férachou D, Ropagnol X and Ozaki T 2016 *J. Opt.* **18** 093004

[33] Zhang X C, Shkurinov A and Zhang Y 2017 *Nat. Photonics* **11** 16–18

[34] Lefaudeux N, Levecq X, Dovillaire G, Theis S and Escolano L 2012 New deformable mirror technology and associated control strategies for ultrahigh intensity laser beam corrections and optimizations *Laser Reson. Microresonators, Beam Control XIV* ed Kudryashov A V, Paxton A H and Ilchenko V S (International Society for Optics and Photonics) p 82360K

[35] 2020 Imagine Optic

[36] 2020 Fastlite URL `http://www.fastlite.com`
[37] 2019 FROG URL `http://www.swampoptics.com/frog.html`
[38] 2020 UltraFast Innovations URL `http://www.ultrafast-innovations.com/`
[39] 2020 Andor URL `https://andor.oxinst.com/`
[40] Maitrallain A, van der Geer B, de Loos M, Manahan G G, Wiggins S M, Li W, Shahzad M, Spesyvtsev R, Battaglia G, Vieux G, Brunetti E and Jaroszynski D 2019 Design of a double dipole electron spectrometer *Laser Accel. Electrons, Protons, Ions V* ed Esarey E, Schroeder C B and Schreiber J (SPIE) p 37
[41] Shahzad M, Reid L R, Spesyvtsev R, Maitrallain A, Holt G K, Zeraouli G, Li W, Vieux G, Brunetti E, Wiggins S M, Gatti G, Luis D D, Volpe L, Fedosejevs R and Jaroszynski D A 2019 Characterisation of a laser plasma accelerator x-ray source size using a Kirkpatrick-Baez microscope *Relativ. Plasma Waves Part. Beams as Coherent Incoherent Radiat. Sources III* vol 11036 ed Jaroszynski D A and Hur M (SPIE) p 25
[42] Tooley M P, Ersfeld B, Yoffe S R, Noble A, Brunetti E, Sheng Z M, Islam M R and Jaroszynski D A 2017 *Phys. Rev. Lett.* **119**
[43] Whittum D H, Sessler A M and Dawson J M 1990 *Phys. Rev. Lett.* **64** 2511–2514
[44] Li F Y, Sheng Z M, Chen M, Yu L L, Meyer-Ter-Vehn J, Mori W B and Zhang J 2014 *Phys. Rev. E - Stat. Nonlinear, Soft Matter Phys.* **90**
[45] Ersfeld B, Bonifacio R, Chen S, Islam M R, Smorenburg P W and Jaroszynski D A 2014 *New J. Phys.* **16** 093025
[46] Ersfeld B, Bonifacio R, Chen S, Islam M R and Jaroszynski D A 2015 Practical considerations for the ion channel free-electron laser *SPIE Opt. + Optoelectron. Relativ. Plasma Waves Part. Beams as Coherent Incoherent Radiat. Sources* vol 9509 ed Jaroszynski D A (International Society for Optics and Photonics) p 95090L
[47] Jaroszynski D A, Bingham R, Brunetti E, Ersfeld B, Gallacher J, Van Der Geer B, Issac R, Jamison S P, Jones D, De Loos M, Lyachev A, Pavlov V, Reitsma A, Saveliev Y, Vieux G and Wiggins S M 2006 *Philos. Trans. R. Soc. A Math. Phys. Eng. Sci.* **364** 689–710
[48] Nakajima K 2008 *Nat. Phys.* **4** 92–93